Journal of Power Sources 195 (2010) 4072–4079

Contents lists available at ScienceDirect

Journal of Power Sources

journal homepage: www.elsevier.com/locate/jpowsour

Preparation and properties of crosslinked sulphonated poly(arylene ether sulphone) blend s for direct methanol fuel cell applications

Jie-Cheng Tsai [a], Chien-Kung Lin [b,*], Jen-Feng Kuo [b], Chuh-Yung Chen [b]

[a] Advanced Propulsion and Power System Research Center, National Cheng-Kung University, Tainan 70148, Taiwan
[b] Department of Chemical Engineering, National Cheng-Kung University, Tainan 70148, Taiwan

ARTICLE INFO

Article history:
Received 23 December 2009
Accepted 26 January 2010
Available online 2 February 2010

Keywords:
Proton exchange membrane
Sulphonated poly(arylene ether sulphone)
Cross-linking
Direct methanol fuel cell
4,4′-Dihydroxy-α-methylstilbene (HMS)

ABSTRACT

HMS-based sulphonated poly(arylene ether sulphone) (HMSSH) is synthesised using 4,4′-dihydroxy-α-methylstilbene (HMS) monomer to introduce an interesting stilbene core as crosslinkable group. Crosslinked blend membranes are obtained by blending the BPA-based sulphonated poly(arylene ether sulphone) (BPASH) with crosslinkable HMS-based sulphonated poly(arylene ether sulphone) by UV irradiation of the blend membrane. Compared to the native BPASH with crosslinked BPASH/HMSSH blend membranes, the crosslinked blend membranes greatly reduce the water uptake and methanol permeability with only a slight reduction in proton conductivity. The crosslinked blend membrane, which has a 6% HMSSH content, has a water uptake of 59%, methanol permeability of 0.75×10^{-6} cm^2 s^{-1}, and proton conductivity of 0.08 S cm^{-1}. A membrane-electrode assembly is used to investigate single-cell performance and durability test for DMFC applications. Both the power density and open circuit voltage are higher than those of Nafion® 117. A maximum power density of 32 mW cm^{-2} at 0.2 V is obtained at 80 °C, which is higher than that of Nafion® 117 (25 mW cm^{-2}).

1. Introduction

The direct methanol fuel cell (DMFC) is an attractive candidate for a mobile energy source because of its advantageous properties such as its highly efficient energy conversion, low operating temperature, simple design and no requirement of a fuel reforming process [1,2]. The proton exchange membrane (PEM) is one of the most important components in a DMFC.

Currently, perfluorinated polymers such as Nafion® are the most common commercially available PEM materials for DMFCs due to high levels of electrochemical stability, mechanical strength and proton conductivity. However, the high cost, high methanol crossover, and difficulty in synthesising and processing have limited the extent of their applications [3]. In particular, the high methanol crossover not only wastes fuel but also causes the loss of cell performance due to it being oxidised without any contribution to power generation and to forming CO as an intermediate, which poisons the cathode [4,5]. Hence, the primary criterion for choosing a PEM is not only high proton conductivity but also low permeability to methanol.

In recent years, several efforts have been made to replace the Nafion® membranes. Among the PEMs being developed, hydrocarbon-based aromatic polymers have been suggested as new PEM materials such as sulphonated poly(ether sulphone) (SPES) [6], sulphonated poly (ether ether ketone) (SPEEK) [7], sulphonated polybenzimidazole (SPBI) [8], and sulphonated polyimide (SPI) [9]. These membranes are prepared either by post-sulphonation or by direct copolymerisation, with at least one of the polymers containing a sulphonic acid group. They require a certain sulphonation level to achieve sufficient proton conductivity. Unfortunately, such a high loading of acidic groups leads to excessive swelling and methanol crossover, which permeates through the ionic channels and clusters of membranes [10,11]. The size of these channels and clusters increases as swelling of the membrane increases. The ease of swelling of the membrane rapidly causes permeation of methanol. Therefore, it becomes necessary to suppress the swelling of the membrane to retain low methanol permeability. In general, suppressing the swelling of the membrane leads to a reduction of proton conductivity.

Crosslinking is a feasible and effective method to suppress water swelling and methanol diffusion of highly sulphonated polymers [12]. To date, many crosslinking methods have been developed, such as ionic crosslinking [13,14] and covalent crosslinking [15–18]. Kerres et al. [19,20] reported various ionic crosslinked membranes by blending SPEEK or SPES with basic polymers. Mikhailenko et al. [21,22] investigated a covalent crosslinking that involved elimination of the sulphonic acid groups of SPEEK. Generally, photo crosslinking is one of the most effective methods to obtain three-dimensional polymer networks [23,24]. Zhong et al.

* Corresponding author. Tel.: +886 6 2757575x62681; fax: +886 6 2344496.
E-mail address: nickel@mail.ncku.edu.tw (C.-K. Lin).

0378-7753/$ – see front matter © 2010 Elsevier B.V. All rights reserved.
doi:10.1016/j.jpowsour.2010.01.057

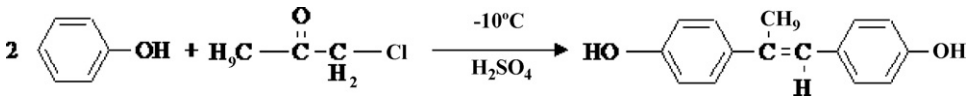

Scheme 1. The reaction for synthesis of the HMS monomer.

[25,26] and Heo et al. [27] studied photo crosslinkable propenyl group of SPEEK and stilbene group of SPES. They found that the photo crosslinking process did not change the ion-exchange capacity of the membrane and that the sulphonic acid groups were stable during the UV irradiation.

SPES has been extensively studied and tested for DMFC applications [28,29] and has been shown to possess many positive attributes such as good mechanical properties, processing capacity, proton conductivity as high as 10^{-2} S cm^{-1} and lower methanol permeability. In this paper, a crosslinked blend membrane was composed of uncrosslinkable SPES and crosslinkable SPES, which was prepared via the direct polymerisation method suggested by McGrath and co-workers [28,29], to introduce an interesting stilbene core as a crosslinkable group on polymer main chain and then crosslinked by UV irradiation. This novel crosslinking method can avoid the consumption of sulphonic acid groups by UV irradiation and the decrease of sulphonic acid concentration by introduction of a crosslinkable sulphonated polymer, benefit the compatibility with blending crosslinkable SPES into uncrosslinkable SPES matrix due to the similar structure of these two fully aromatic copolymers, and hence form a more compact network structure, which effectively suppresses the swelling and methanol permeability.

2. Experimental

2.1. Materials

Fuming sulphuric acid (30% SO_3) and concentrated sulphonic acid (95–98%) were obtained from Aldrich Chemical Corp. Chloroacetone was purchased from Janssen Chimica Corp. Phenol and sodium hydroxide were obtained from Shimakyo's Pure Chemicals Corp. 4,4′-Dichlorodiphenylsulphone (DCDPS), N-methylpyrrolidone (NMP), dimethylacetamide (DMAc), toluene and bisphenol A (BPA) were purchased from Acros Corp. Methanol and isopropyl alcohol (IPA) were obtained from Mallinckrodt Co. Nafion® 117 and Nafion® solution (5%, sulphonic acid form) were purchased from E. I. DuPont de Nemours & Co. Nafion® 117 was treated to completely remove all impurities by boiling in 3% H_2O_2, 0.5 M H_2SO_4 and then in deionised water.

2.2. Monomer synthesis

2.2.1. 4,4′-Dihydroxy-α-methylstilbene (HMS)

HMS was synthesised by the procedure outlined by Zaheer et al. and in our previous research [30–33]. Chloroacetone and phenol were poured into a four-necked Pyrex reactor with stirring at −10 °C. Concentrated sulphonic acid was then added dropwise to the solution (Scheme 1). mp 183–184 °C, yield: 21%.

^{1}H NMR (DMSO-d_6): δ = 2.1 (S, 3H, –CH_3), 6.6 (S, 1H, –C=CH–), 6.7 (d, 4 aromatic protons, *o* to –OH), 7.1 (d, 2 aromatic protons, *o* to –CH_3), 7.3 (d, 2 aromatic protons, *o* to =CH), 9.4 (s, 2H,–OH).

2.2.2. Sulphonated dichlorodiphenolsulphone (SDCDPS)

The synthesis of SDCDPS was performed according to the procedure reported by McGrath and co-workers [28,29], yield: 82%.

^{1}H NMR (DMSO-d_6): δ = 7.6 (d, 2 aromatic protons, *m* to –SO_2), 7.8 (dd, 2 aromatic protons, *o* to –SO_2), 8.3 (d, 2 aromatic protons, *o* to –SO_3Na).

2.3. Polymer synthesis (HMSSH and BPASH)

SPESs were synthesised via an aromatic nucleophilic substitution reaction in NMP with toluene as an azeotroping agent (Scheme 2). The degree of sulphonation is the number of disulphonic acid groups per repeating unit. In the reaction, the degree of sulphonation of BPASH and HMSSH was 40 mol%. The polymerisation was carried out in a 150-mL three-necked flask equipped with a mechanical stirrer, nitrogen inlet, and a Dean–Stark trap as a reflux condenser. HMS (or BPA), SDCDPS, and DCDPS monomers were added, as well as an excess of anhydrous potassium carbonate. NMP and toluene were then charged into the flask. The reaction mixture was refluxed at 150 °C for 4 h to dehydrate until water was removed from the reaction. The temperature was slowly raised to 190 °C for 19 h. The reaction was then cooled to room temperature. The polymer solution was diluted with DMAc, filtered to remove the sodium salt, and precipitated into water. The resulting polymer was isolated, washed repeatedly with deionised water to completely remove the residual sodium, and dried in a vacuum oven at 120 °C for 24 h.

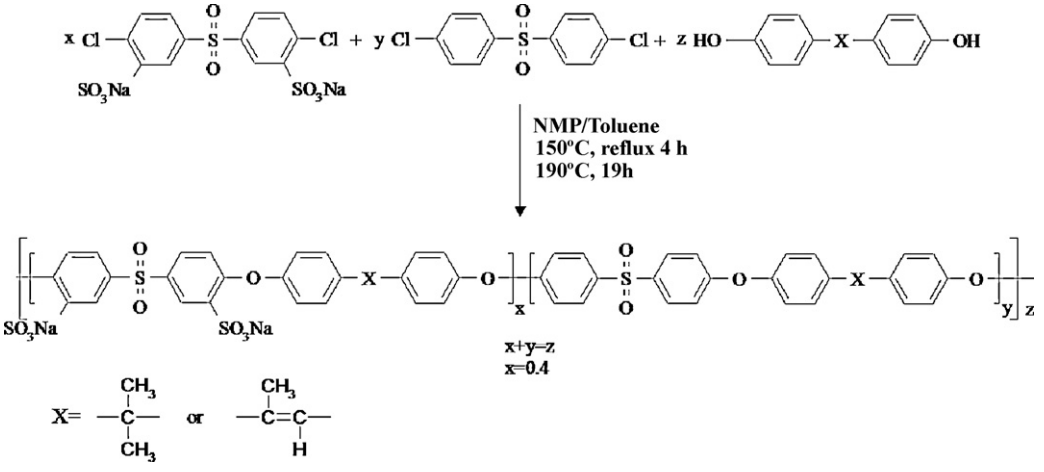

Scheme 2. The synthesis of BPASH and HMSSH was prepared via an aromatic nucleophilic substitution reaction.

2.4. Membrane preparation

The crosslinked BPASH/HMSSH blend membrane was prepared by a solution casting method [25–27]. First, the BPASH and HMSSH were dissolved in DMAc to obtain a 15 wt.% solution. The weight ratios of the blend varied from 3% to 9% crosslinkable HMSSH. Next, benzophenone and triethylamine as the photo-initiator system were added to the solution. The resulting mixture was continuously stirred until a transparent solution was obtained. The mixture was then cast onto a glass dish and dried under vacuum at 80 °C. To obtain the crosslinked blend membrane, the dried membrane was irradiated for 20 min with a 600-W UV light. The crosslinked blend membrane in sodium form was treated with 0.5 M H_2SO_4 at boiling temperature for 2 h to give the acid form (method 2) [34]; afterwards, the membrane was washed with deionised water to remove excess acid and was stored in deionised water. It can be observed that all membranes used here to prepare the crosslinked blend membranes have almost similar sulphonic acid contents and no sulphonic acid group loss in the crosslinking reaction. The crosslinked blend membrane thus prepared was designated as BPASH/HMSSH-X, where X is the HMSSH content in the membrane.

2.5. Proton nuclear magnetic resonance (^{1}H NMR)

The BPASH and HMSSH were obtained from DMSO-d_6 solution (10 wt.%) at room temperature. The ^{1}H NMR spectra were obtained with a Varian Unity 600 spectrometer and a Bruker AMX 600 MHz spectrometer.

2.6. Fourier transform infrared spectroscopy (FT-IR)

An FT-IR spectrometer with an attenuated total reflection (ATR) attachment was used to confirm the presence of functional groups on the membranes. Spectra were obtained with a Bio-Rad FTS-40A spectrometer in the wavelength range of 700–4000 cm^{-1}. Each spectrum is the average of 48 scans with a resolution of 4 cm^{-1}.

2.7. Thermogravimetric analysis (TGA)

All membranes were heated at 120 °C for 30 min in a furnace to remove moisture. The dynamic TGA experiments were done under a nitrogen atmosphere with a TGA Q50 thermal analyser (TA Instruments, WI) from 100 °C to 700 °C at a heating rate of 20 °C min^{-1}.

2.8. Differential scanning calorimetry (DSC)

A DuPont DSC 2910 differential scanning calorimeter was used for the analysis of the thermal transition behaviour of the membranes from 30 °C to 250 °C at a heating rate of 10 °C min^{-1} under a nitrogen atmosphere.

2.9. Water uptake by membranes

Membranes were dried to constant weight under vacuum at 120 °C. The water uptake was measured by immersing the membranes in deionised water and heating from 30 °C to 80 °C. The weight of equilibrium water uptake was determined as:

$$\text{water uptake} = \frac{W_{wet} - W_{dry}}{W_{dry}} \times 100\% \quad (1)$$

where W_{wet} and W_{dry} are the weights of the wet and dry membrane, respectively.

2.10. Methanol permeability

The methanol permeability of the membranes was determined using a diaphragm diffusion cell. The membranes were equilibrated in deionised water overnight with stirring. The initial concentration of methanol on one side of the cell (compartment A) was 2 M, while the other side of the cell (compartment B) contained deionised water. The increase in the concentration of methanol with time was determined by gas chromatography. The methanol permeability was calculated from the slope of a least-squares linear fit:

$$C_B(t) = \frac{A}{V_B}\frac{P}{L}C_A(t - t_0) \quad (2)$$

where A is the effective membrane area, L is the membrane thickness, C_A and C_B are the initial concentrations of methanol in compartments A and B, respectively, and V_B is the volume of compartment B.

2.11. Proton conductivity measurement

The proton conductivity cell was immersed in water at a constant temperature from 30 °C to 80 °C. The conductivity of the membranes in the in-plane direction was determined with an electrochemical cell. A stainless steel blocking electrode was used for the measurement. AC impedance analysis was done with Autolab PGSTAT 30 equipment (Eco Chemie B. V., Netherlands). The frequency response analysis (FRA) software used an oscillation potential of 10 mV from 100 kHz to 10 Hz. The proton conductivity of membranes was determined as follows:

$$\sigma = \frac{l}{RA} \quad (3)$$

where σ is the proton conductivity, l is the distance between the electrodes, R is the membrane resistance obtained by impedance analysis, and A is the membrane area.

2.12. Single-cell performance

Nafion® 117 and the crosslinked blend membranes were used as proton exchange membranes in a fuel cell, and the catalysts for the anode and the cathode were applied to carbon paper by spreading. The anode and cathode consisted of commercial 20 wt% Pt/Ru (1:1) in Vulcan carbon (E-TEK) with Pt loadings of 1.2 mg cm^{-2} and 0.6 mg cm^{-2}, respectively. The membrane-electrode assemblies (MEAs) were fabricated by uniaxially hot-pressing the anode and cathode onto the membrane at 135 °C for 90 s. Methanol (2 M) was supplied to the anode with a micro-pump at 2 mL min^{-1}, while the cathode was supplied with dry O_2 at a rate of 100 mL min^{-1}. Single-cell performance was evaluated using a DMFC unit with a cross-section area of 4 cm^2.

3. Results and discussion

3.1. Copolymer characteristics

The ^{1}H NMR spectra were used to identify the molecular structure and to confirm the compositions of the synthesised HMSSH and BPASH [29,35]. Fig. 1(a) and (b) shows the ^{1}H NMR spectrum of HMSSH and BPASH dissolved in DMSO-d_6. By integration and rationing of known reference protons in the polymer, the relative compositions of the sulphonated polymers can be determined. As shown in Fig. 1(a), the two protons ortho to the sulphone and adjacent to the sulphonate group (proton 'k', ~8.30 ppm) on the sulphonated dihalide monomer were well separated from aromatic protons of the HMS monomer (proton 'b, b'', ~7.63 and 7.45 ppm) on the non-sulphonated segment. These indicate that the

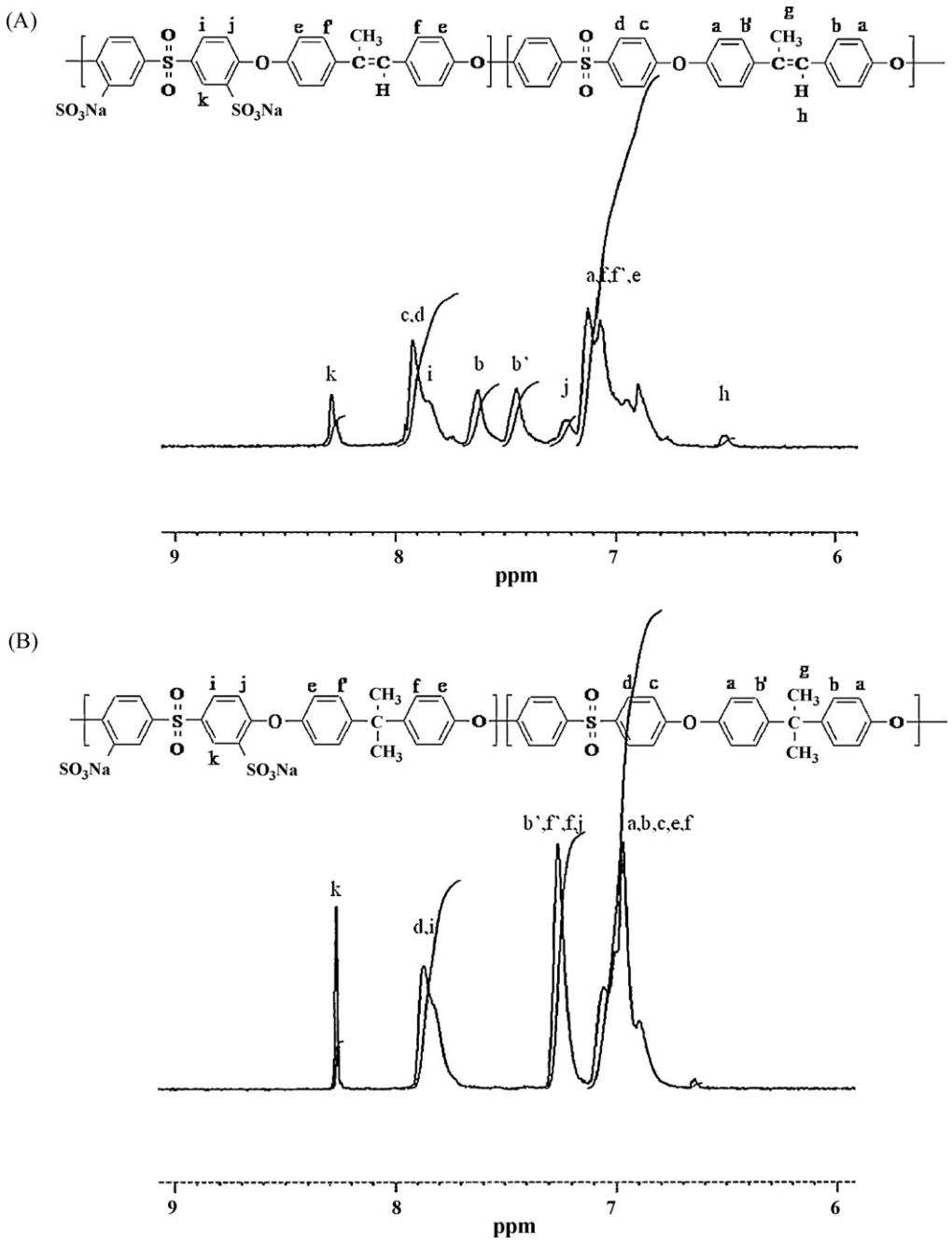

Fig. 1. The ^{1}H NMR spectra for (a) HMSSH and (b) BPASH.

sulphonate groups were successfully introduced into the copolymers via a nucleophilic step polymerisation without any side reactions. In this study, by integration and ratio measurement of these peaks, the degree of sulphonation of HMSSH and BPASH was 0.40. HMSSH can act a crosslinker and provide sufficient sulphonate groups in crosslinked blend membranes.

The FT-IR ATR technique was used to analyse the functional groups in the polymer structure. Fig. 2(a)–(f) shows the FT-IR ATR spectra of uncrosslinked and crosslinked BPASH/HMSSH blend membranes. The strong characteristic peaks at 1030 cm^{-1} and 1098 cm^{-1} were assigned to symmetric and asymmetric stretching of sulphonate groups, respectively, which were observed for BPASH and HMSSH loaded with sulphonate groups [36,37]. The absorption of the Ar–O–Ar linkage in the polymer backbone appears at 1008 cm^{-1}. The intensity of the absorption peak at 1626 cm^{-1} assigned to trans C=C double bonds of crosslinkable HMSSH obviously decreased by UV irradiation, which indicates the occurrence of crosslinking. Moreover, the crosslinked blend membranes became insoluble in DMAc, DMF, DMSO and NMP solvents after full thermal treatment, which also indicates the formation of crosslinkage among the HMSSH polymer chains.

3.2. Thermal characteristics

The thermal stability of membranes was investigated by TGA. Fig. 3 shows the 5% (w/w) loss temperature (T_{d5}) of native BPASH and crosslinked BPASH/HMSSH blend membranes with various contents of HMSSH. The native BPASH and HMSSH are well known to be thermally stable polymers and show T_{d5} of 300 °C and 318 °C. For all of the membranes, two major weight loss stages were

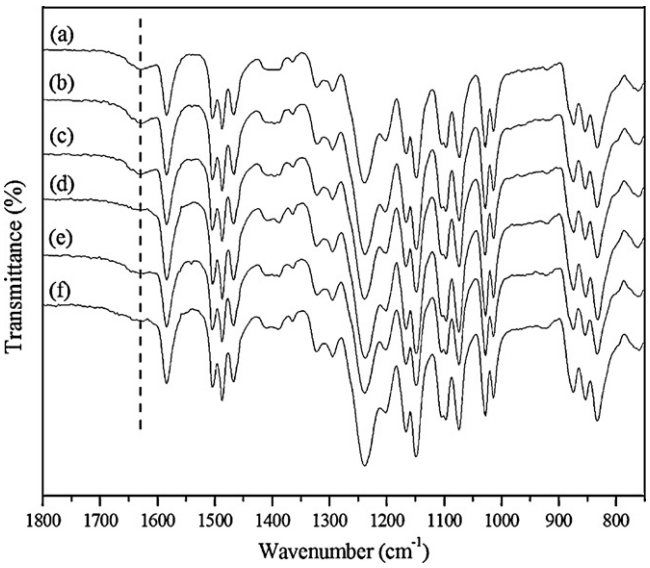

Fig. 2. The FT-IR ATR spectra of uncrosslinked (a) BPASH/HMSSH-3%, (b) BPASH/HMSSH-6%, (c) BPASH/HMSSH-9%, and crosslinked (d) BPASH/HMSSH-3%, (e) BPASH/HMSSH-6%, (f) BPASH/HMSSH-9%.

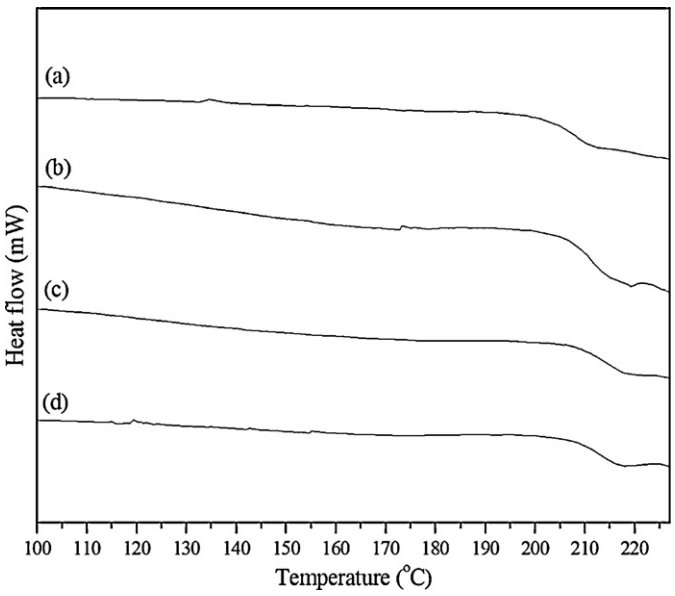

Fig. 4. The transition temperature of (a) native BPASH, (b) BPASH/HMSSH-3%, (c) BPASH/HMSSH-6% and (d) BPASH/HMSSH-9%.

observed [25]. The first weight loss was assigned to the loss of sulphonic acid groups by evolution of SO and SO_2. The second degradation step contributed to the decomposition of the polymer main chain. As shown in Fig. 3, with the increase of crosslinkable HMSSH content from 3 wt% to 9 wt%, T_{d5} values was all found to be at around 300 °C. The effect of crosslinking on the thermal stability was not pronounced. In crosslinked blend membranes, two major factors may compete with each other to affect the thermal stability. First, the crosslinking at the stilbene group destroys the liquid crystal core of HMS segment on the main chain; consequently, the thermal stability decreases. In contrast, when the polymer chains are crosslinked, the BPASH cohesion and polymer network increased, which resulted in enhancement of thermal stability. The former factor may be dominant in this study. However, the thermal stability of crosslinked blend membranes is sufficient to serve as the PEM in DMFC applications.

Differential scanning calorimetry analysis was used to characterise the thermal transition for the native BPASH and crosslinked BPASH/HMSSH blend membranes. Fig. 4 shows the glass transition temperatures of the membranes. It clearly shows that only one glass transition temperature (T_g) is present. These DSC data show the T_g to be at around 210 °C. In general, the T_g of the crosslinked membrane is higher than that of the uncrosslinked membrane. The increase of T_g is contributed to the increase of polymer cohesion and the formation of crosslinking network structure. In this study, HMSSH has a stilbene core as a crosslinkable group which is also a mesogen group of liquid crystal (LC) of HMS segment on the polymer main chain. The LC molecules are oriented in different directions. Within a domain, however, the molecules are well ordered. The crosslinking at the stilbene group destroys the ordering; consequently, the T_g show the similar transition at around 210 °C.

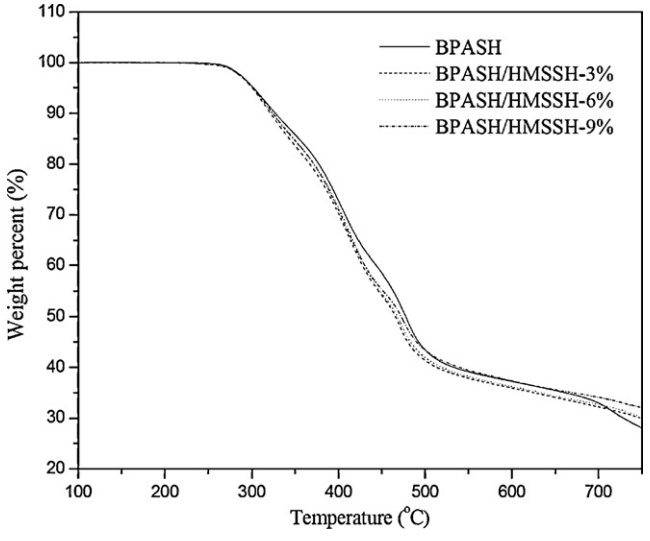

Fig. 3. The thermogravimetric curves of native BPASH and crosslinked BPASH/HMSSH blend membranes.

3.3. Water uptake

It is well known that the proton conductivity and methanol permeability of the membrane are strongly related to the presence of water. An adequate level of water uptake is needed to maintain good proton conductivity; however, excessive water uptake will result in mechanical frailty, low dimensional stability, and high methanol permeability of membranes, all of which will lead to poor performance, especially in DMFC applications. Fig. 5 shows the water uptake of native BPASH and crosslinked BPASH/HMSSH blend membranes with various contents of HMSSH as a function of temperature. Compared with the native BPASH membrane, water uptake of the crosslinked blend membranes can be adjusted over a broad range. The BPASH absorbed 73% water at 30 °C, whereas the water uptake of the BPASH/HMSSH-3% membrane was only 63%. This result clearly indicates that the presence of stilbene bands in the blend membranes led to crosslinking, which eventually hindered their mobility and the absorption of water in the membrane. As the crosslinkable HMSSH content increased, the water uptake of the membrane further decreased, down to 59% and 52% for BPASH/HMSSH-6% and BPASH/HMSSH-9%, respectively. Obviously, crosslinking is a useful method for constraining the water uptake because it increases the compactness of molecules and restricts the mobility of polymer chains. The crosslinked blend membranes had denser structures and smaller free volumes than did the native BPASH membrane, which resulted in fewer and smaller transfer

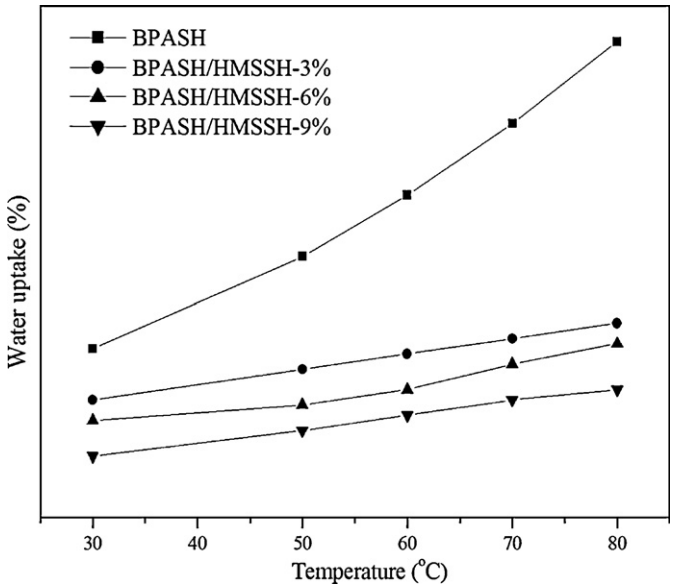

Fig. 5. The water uptake of native BPASH and crosslinked BPASH/HMSSH blend membranes.

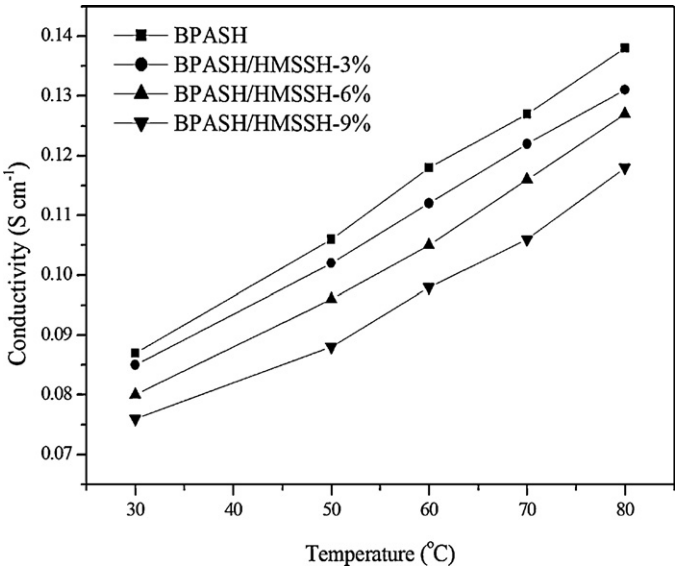

Fig. 6. The proton conductivity for native BPASH and crosslinked BPASH/HMSSH blend membranes.

channels and ionic clusters [25,26]. Furthermore, elevating temperature can increase the mobility of polymer chains and the free volume for water adsorption, which leads to an increase in water absorbency of membranes. It was obvious that as the amount of crosslinker increased, the water uptake became less dependent on temperature from 133% to 78%, 74%, and 65% for 3%, 6%, and 9% of crosslinker. This indicates that crosslinking could suppress the problem of excessive water sorption of native BPASH membrane at elevated temperatures.

3.4. Methanol permeability

The methanol permeability of the membrane is an important property for DMFCs. A membrane with low methanol permeability is required because methanol diffusing from the anode to the cathode causes a drastic reduction of cell performance and fuel efficiency. Methanol diffusion across the membranes is mainly related to the water uptake and the microstructure of the membranes because methanol passes through the transfer channels and ionic clusters. It is obvious that crosslinking effectively suppressed the methanol permeability, which decreased with increasing crosslinker amounts for crosslinked blend membranes. Changes in methanol permeability and water uptake of the crosslinked blend membranes were similar: with increasing amounts of crosslinker, the methanol permeability of the membranes drastically decreased. The methanol permeability of the native BPASH membrane was 1.64×10^{-6} cm^2 s^{-1} at 30 °C, whereas those of the crosslinked BPASH/HMSSH blend membranes with 3%, 6%, and 9% crosslinker were 1.02×10^{-6} cm^2 s^{-1}, 0.75×10^{-6} cm^2 s^{-1}, and 0.54×10^{-6} cm^2 s^{-1}, respectively, which effectively suppressed membrane water absorption and inhibited the methanol passage and hence resulted in the reduction of methanol permeability. For comparison, the methanol permeabilities of all of the crosslinked blend membranes were lower than that of Nafion® 117 (2.38×10^{-6} cm^2 s^{-1}).

3.5. Proton conductivity

The performance of a DMFC is mainly determined by proton conductivity and methanol permeability. In general, there are several factors, such as the proton concentration, polymer structure, morphology, proton mobility, and water content, that affect the level of proton conductivity. Fig. 6 shows the proton conductivities of native BPASH and crosslinked BPASH/HMSSH blend membranes as functions of temperature. The proton conductivity was slightly reduced. BPASH showed a proton conductivity of 0.087 S cm^{-1}, whereas the crosslinked blend membranes exhibited proton conductivities of 0.085 S cm^{-1}, 0.080 S cm^{-1}, and 0.076 S cm^{-1} with an increase of crosslinker from 3% to 9% at 30 °C.

Although this led to a slight reduction in proton conductivity, the proton conductivity of the crosslinked blend membranes was maintained at the level of 10^{-2} S cm^{-1}, which is comparable to that of Nafion® 117 (0.098 S cm^{-1}). The decrease in proton conductivity could have resulted from the crosslinkage restricting morphological structure and decreasing the free volume in the membrane, which may have resulted in fewer and smaller hydrophilic channels and ionic clusters for water uptake, hindering the transfer of hydrated protons in the water phase. In addition, it can be observed that temperature played an important role on the proton conductivity and that all membranes exhibited positive temperature-conductivity dependency. When the temperature of the fully hydrated environment increased to 80 °C, the proton conductivity of all membranes significantly increased with similar trends. The proton conductivity of crosslinked blend membranes gradually increased to 0.131 S cm^{-1}, 0.127 S cm^{-1}, and 0.118 S cm^{-1} for 3%, 6%, and 9%, respectively. This is due to the elevation of temperature increasing the mobility of water and polymer chains, which consequently enhanced the transport of hydrated protons. In addition, the increase of temperature led to increased water uptake. More water as the proton transport medium might allow protons to move more easily through the hydrophilic channels and ionic clusters, hence contributing to the improvement of proton conductivity. The crosslinking extent here was controlled by adjusting the crosslinker content. Therefore, it is possible to achieve a relative balance of methanol diffusion and proton conductivity by controlling the crosslinker content.

3.6. Single-cell performance

Nafion® 117, BPASH and crosslinked BAPSH/HMSSH blend membranes were used in DMFC. Fig. 7 shows the performance of BAPSH/HMSSH-6% with polarisation as a function of temperature. The increase in temperature from 30 °C to 80 °C significantly

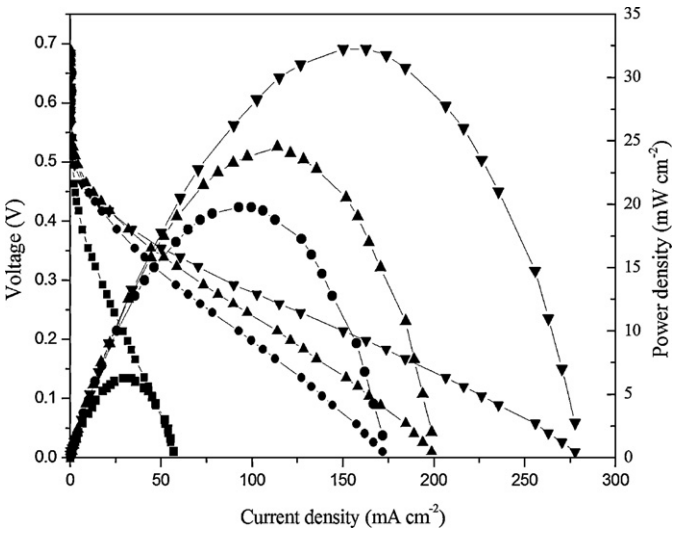

Fig. 7. The performance curves of BPASH/HMSSH-6% at (a) (■) 30 °C, (●) 60 °C, (▲) 70 °C and (▼) 80 °C.

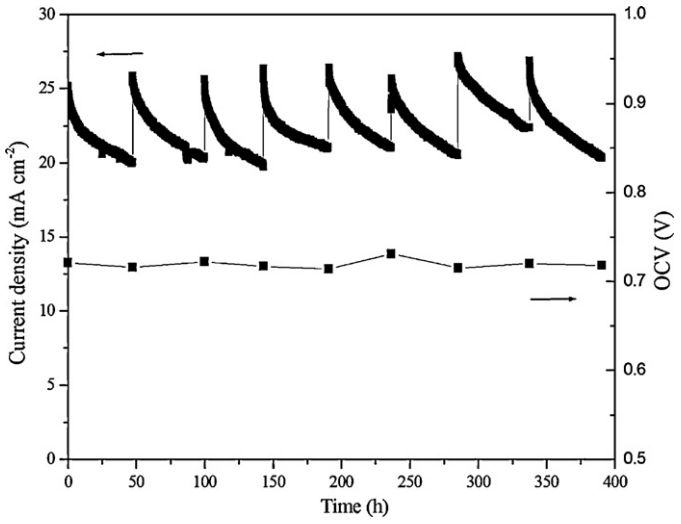

Fig. 9. The single-cell durability test of BPASH/HMSSH-6% membrane.

improved the cell performance, and the maximum power density at 0.2 V of BAPSH/HMSSH-6% was 6–32 mW cm^{-2}. Fig. 8 shows the performance with polarisation (a) and power density (b) as functions of current density with various contents of crosslinker. All of the characteristic curves displayed similar polarisation behaviour. In the region of low current density, activation control caused a large drop of potential, which was further decreased by the intrinsic ohmic resistance at intermediate current density. Single cells with any of the crosslinked blend membranes had a higher open circuit voltage (OCV 0.65–0.68 V) than did Nafion® 117 (OCV 0.59 V). The higher OCV clearly indicates that the introduction of crosslinker significantly decreased the rate of methanol crossover in the DMFC applications due to the relatively low methanol permeability. Although the conductivity of the crosslinked blend membranes was lower than that of Nafion®, the DMFC performance can be improved by a reduction in methanol crossover. As the HMSSH content of crosslinked blend membrane was increased to 9%, the ohmic resistance increased, and the performance decreased. The crosslinked blend membrane with a content of 6% crosslinker had the highest power density (32 mW cm^{-2}), which was better than that of the other crosslinked blend membranes and of Nafion® 117 (25 mW cm^{-2}). However, the low loading voltage at around 0.5 V, may be come from the electrode structure. To optimize the electrode structure further, there are many parameters, like the composition of the catalyst itself (Pt or Pt/Ru or other alloys), catalyst loading (high or low), ionomer content in the catalyst layer (high or low), porosity of the electrode (typical membrane-electrode assemblies or catalyst coating on membrane), etc. Fig. 9 shows the durability test for BPASH/HMSSH-6% as functions of time to characterise the stability of the used membrane. The current density at a voltage of 0.4 V and the OCV of the crosslinked blend membrane were recorded with 1.5 M methanol concentration over 390 h at 60 °C. No obvious decrease in current density and OCV were at the time scale of experiment. It is suggested that the crosslinked blend membrane had good stability and resisted the OCV decay rate under fuel cell conditions.

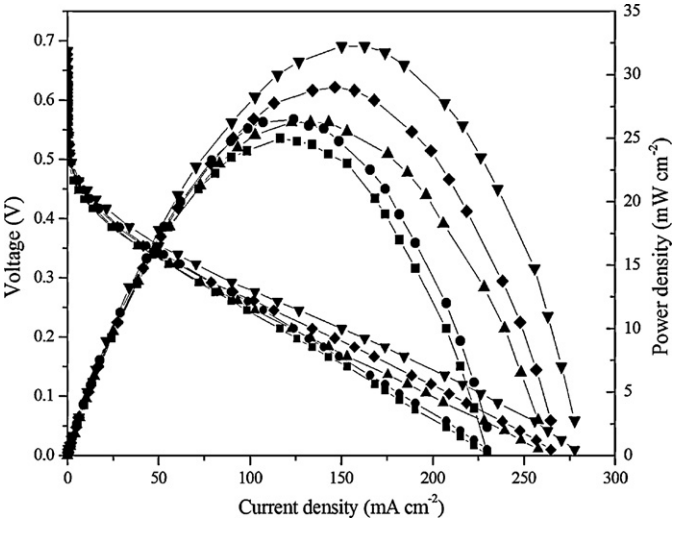

Fig. 8. The performance curves of (■) Nafion® 117, (●) BPASH, (▲) BPASH/HMSSH-3%, (▼) BPASH/HMSSH-6% and (♦) BPASH/HMSSH-9% at 80 °C.

4. Conclusion

Crosslinked blend membranes are obtained by blending the crosslinkable HMSSH with BPASH by UV irradiation of the blend membrane, which can avoid the consumption and dilution of sulphonic acid groups and benefit the compatibility with blending HMSSH into BPASH matrix. The studies showed that compared with the pristine BPASH, the incorporation of crosslinker in BPASH decreased the methanol permeability of the membrane, significantly suppressed methanol crossover, decreased the water uptake, and retained reasonable thermal properties. Although the conductivity was decreased, the methanol crossover of the crosslinked blend membranes could be decreased as a result of reduced hydrophilic channels and ionic clusters for water uptake. The experimental results revealed that the crosslinked blend membranes with 6% HMSSH content exhibited the higher OCV and superior single-cell performance compared with that of the other crosslinked blend membranes and of Nafion® 117. The promising observed single-cell performance and durability test suggest that crosslinked blend membranes warrant serious consideration for use in future DMFC applications.

Acknowledgements

The authors are extremely grateful to Ms P.Y. Lin and Professor W.H. Lai for their crucial contribution to the ^{1}H NMR experiments and the single-cell performance test.

References

[1] V. Neburchilov, J. Martin, H. Wang, J. Zhang, J. Power Sources 169 (2007) 221–238.
[2] M.A. Hickner, H. Ghassemi, Y.S. Kim, B.R. Einsla, J.E. McGrath, Chem. Rev. 104 (2004) 4587–4612.
[3] J.A. Kerres, J. Membr. Sci. 185 (2001) 3–27.
[4] A. Heinzel, V.M. Barragan, J. Power Sources 84 (1999) 70–74.
[5] D.R. Rolison, P.L. Hagans, K.E. Swider, J.W. Long, Langmuir 15 (1999) 774–779.
[6] W.L. Harrison, M.A. Hickner, Y.S. Kim, J.E. McGrath, Fuel Cells 5 (2005) 201–212.
[7] L. Li, J. Zhang, Y.X. Wang, J. Membr. Sci. 226 (2003) 159–167.
[8] M. Rikukawa, K. Sanui, Prog. Polym. Sci. 25 (2000) 1463–1502.
[9] N. Asano, M. Aoki, S. Suzuki, K. Miyatake, H. Uchida, M. Watanabe, J. Am. Chem. Soc. 128 (2006) 1762–1769.
[10] C. Manea, M. Mulder, J. Membr. Sci. 206 (2002) 443–453.
[11] K.D. Kreuer, J. Membr. Sci. 185 (2001) 29–39.
[12] J.A. Kerres, Fuel Cells 5 (2005) 230–247.
[13] L. Jorissen, V. Gogel, J. Kerres, J. Garche, J. Power Sources 105 (2002) 267–273.
[14] R. Wycisk, J. Chisholm, J. Lee, J. Lin, P.N. Pintauro, J. Power Sources 163 (2006) 9–17.
[15] J. Chen, Y. Maekawa, M. Asano, M. Yoshida, Polymer 48 (2007) 6002–6009.
[16] W. Zhang, V. Gogel, K.A. Friedrich, J. Kerres, J. Power Sources 155 (2006) 3–12.
[17] Y. Yin, O. Yamada, K. Tanaka, K. Okamoto, Polym. J. 38 (2006) 197–219.
[18] C.H. Lee, H.B. Park, Y.S. Chung, Y.M. Lee, B.D. Freeman, Macromolecules 39 (2006) 755–764.
[19] J. Kerres, W. Zhang, A. Ullrich, C.M. Tang, M. Hein, V. Gogel, T. Frey, L. Jorissen, Desalination 147 (2002) 173–178.
[20] J. Kerres, A. Ullrich, F. Meier, T. Haring, Solid State Ionics 125 (1999) 243–249.
[21] S.D. Mikhailenko, G.P. Robertson, M.D. Guiver, S. Kaliaguine, J. Membr. Sci. 285 (2006) 306–316.
[22] S.D. Mikhailenko, K. Wang, S. Kaliaguine, P. Xing, G.P. Robertson, M.D. Guiver, J. Membr. Sci. 233 (2004) 93–99.
[23] Q. Guo, P.N. Pintauro, H. Tang, S. O'Connor, J. Membr. Sci. 154 (1999) 175–181.
[24] S. Fujiyama, J. Ishikawa, T. Omi, S. Tamai, Polym. J. 40 (2008) 17–24.
[25] S. Zhong, C. Liu, H. Na, J. Membr. Sci. 326 (2009) 400–407.
[26] S. Zhong, X. Cui, H. Cai, T. Fu, C. Zhao, H. Na, J. Power Sources 164 (2007) 65–72.
[27] K.B. Heo, H.J. Lee, H.J. Kim, B.S. Kim, S.Y. Lee, E. Cho, I.H. Oh, S.A. Hong, T.H. Lim, J. Power Sources 172 (2007) 215–219.
[28] W.L. Harrison, M.A. Hickner, Y.S. Kim, J.E. McGrath, Fuel cell 5 (2005) 201–212.
[29] W.L. Harrison, F. Wang, J.B. Mecham, V.A. Bhanu, M. Hill, Y.S. Kim, J.E. McGrath, J. Polym. Sci. Part A: Polym. Chem. 41 (2003) 2264–2276.
[30] S.H. Zaheer, B. Bhushan, Nature 171 (1953) 746–747.
[31] V. Percec, T.D. Shaffer, H. Nava, J. Polym. Sci. Polym. Lett. Ed. 2 (1984) 637–647.
[32] C.K. Lin, J.F. Kuo, C.Y. Chen, Eur. Polym. J. 37 (2001) 303–313.
[33] J.C. Tsai, J.F. Kuo, C.Y. Chen, J. Power Sources 174 (2007) 103–113.
[34] Y.S. Kim, F. Wang, M. Hickner, S. McCartney, Y.T. Hong, W. Harrison, T.A. Zawodzinski, J.E. McGrath, J. Polym. Sci. Part B: Polym. Phys. 41 (2003) 2816–2828.
[35] S.D. Park, Y.J. Chang, J.C. Jung, W. Lee, H. Chang, H. Kim, Macromol. Symp. 249–250 (2007) 202–208.
[36] F. Wang, M. Hickner, Y.S. Kim, T.A. Zawodzinski, J.E. McGrath, J. Membr. Sci. 197 (2002) 231–242.
[37] K.B. Wiles, F. Wang, J.E. McGrath, J. Polym. Sci. Part A: Polym. Chem. 43 (2005) 2964–2976.